



HOPF BIFURCATION ANALYSIS OF A ROTOR/SEAL SYSTEM

Q. DING

Department of Mechanics, Tianjin University, Tianjin 300072, People's Republic of China

AND

J. E. COOPER AND A. Y. T. LEUNG

School of Engineering, The University of Manchester, Manchester M13 9PL, England

(Received 7 August 2000, and in final form 9 February 2001)

The Hopf bifurcation behaviour of a symmetric rotor/seal system was investigated using Muszynska's non-linear seal fluid dynamic force model. For a perfectly balanced system, the instability from certain critical equilibrium positions is proved to be the result of Hopf bifurcation and only the supercritical type is found for a specific rotor system using Poore's algebraic criteria. Hence, a stable periodic orbit bifurcates from the critical equilibrium position after the threshold speed is exceeded. Due to the dimensionless whirl frequency being found to be close to $\frac{1}{2}$ over quite a large range of system parameters, the periodically perturbed Hopf bifurcation in $\frac{1}{2}$ subharmonic resonance is dealt with for an imbalanced rotor system. The bifurcation of the averaged system, obtained using the centre manifold procedure and averaging method, is analyzed. The results show that non-synchronized whirl of the imbalanced rotor can either be a quasi-periodic motion resulting from a Hopf bifurcation, or a half-frequency whirl from period doubling bifurcation, determined by the structure parameters of the system and operation conditions. Numerical simulation verifies the analytical results.

© 2002 Elsevier Science Ltd. All rights reserved.

1. INTRODUCTION

Since steam turbines and turbo-compressors are now designed for high performance, seal fluid flow can cause rotating machines to exhibit whirl/whip instability under certain operating conditions [1]. The instability problem of rotor/seal system has been extensively analyzed by linearizing the seal fluid forces around the equilibrium position of the rotor to get the so-called dynamic coefficients of seal [2, 3]. However, the nature of the whirling motion after onset of instability cannot be analyzed using the linearized method. But non-linear analysis of the problem is still rare due to the difficulties in obtaining the analytical non-linear model of seal fluid force from the complicated fluid dynamics. To overcome this difficulty, a simple model of non-linear fluid dynamic forces generated in the seal (as well as in the bearing) was proposed by Muszynska, based on the results of a series of experiments [4–6]. A parameter called the fluid average circumferential velocity ratio is used to describe the characteristic of the fluid motion as a whole. The fluid film radial stiffness, damping and inertia effects are described by non-linear functions of the rotor eccentricity ratio inside the seal. The model has been used in analyses, such as in antiswirl

arrangements to prevent rotor/seal instability, which suggested that the model is correct and effective [7].

In most cases, steady state instabilities occurring in mechanical systems are the result of Hopf bifurcations. For rotor systems, such a case means that energy is transferred from rotating motion into periodic whirl motion, so the latter can be sustained and is referred to as a limit circle. Determining the direction of bifurcation and the stability of the limit circle is clearly important for understanding the nature of the bifurcated motion (whirling). Much work has been devoted to finding simplified techniques in this respect [8]. Among them, a simple algebraic criterion established by Poore is perhaps the most useful [9]. The method does not require the functions on the right side of a real n -dimensional, first order system of autonomous ordinary differential equation (ODE) to be in any special form, nor is it necessary to transform the functions to new variables. So use of the formula is relatively straightforward. Myers used Poore's algebraic criteria to investigate the oil whirl of a rotor/bearing system [10]. Both super- and subcritical bifurcations were found in different regions of parameter space of the system.

In rotor systems, imbalance of the rotor is inevitable but often at a small level. The rotating inertial force provides a periodic excitation to the rotor in any transverse direction. So a periodic perturbation to the Hopf bifurcation motion exists. Several authors [11–13] have investigated the periodically perturbed Hopf bifurcation. The bifurcation modes are described in detail by Gambaudo [12] using the Poincaré mapping method. In rotor dynamics, Shaw and Shaw [14], on the basis of reference [10], studied the effect of imbalance on oil whirl of rotor/bearing system by the centre manifold procedure and the mapping method, and many bifurcation modes were obtained.

In this paper, a symmetric rotor/seal system is considered and Muszynska's non-linear seal fluid dynamic force model is used. Firstly, the Hopf bifurcation of a perfectly balanced system is studied using Poore's algebraic criteria to predict the direction of bifurcation and the stability of the whirling orbit. Then, the periodically perturbed Hopf bifurcation in $\frac{1}{2}$ subharmonic resonance is investigated with centre manifold theory and the averaging method in the neighbourhood of the threshold speed. The averaged equation is analyzed to find the types of occurrence of the bifurcation from the trivial solution, which indicates the relationship of the type of the non-synchronised whirl with the system parameters and operation conditions. The analytical results are verified by numerical simulation.

2. EQUATIONS OF MOTION

A model of the fluid dynamic forces F generated in seal (as well as in bearing) of turbo-machinery, based on results of a series of experiments, was proposed by Muszynska [4–6] as

$$\begin{bmatrix} F_x \\ F_y \end{bmatrix} = - \begin{bmatrix} K - m_f \tau^2 \omega^2 & \tau \omega D \\ -\tau \omega D & K - m_f \tau^2 \omega^2 \end{bmatrix} \begin{bmatrix} x \\ y \end{bmatrix} - \begin{bmatrix} D & 2\tau \omega m_f \\ -2\tau \omega m_f & D \end{bmatrix} \begin{bmatrix} \dot{x} \\ \dot{y} \end{bmatrix} - \begin{bmatrix} m_f & 0 \\ 0 & m_f \end{bmatrix} \begin{bmatrix} \ddot{x} \\ \ddot{y} \end{bmatrix}, \quad (1)$$

where x and y are the displacements of the shaft centre, and ω the angular rotating speed of the rotor. τ , the fluid average circumferential velocity ratio, is the key parameter which describes the characteristic of the fluid motion as a whole. K , D and m_f are the fluid film

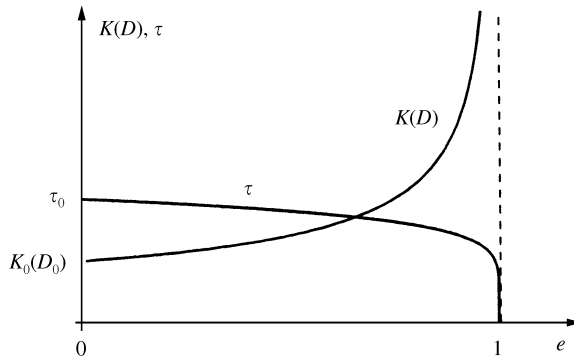


Figure 1. Parameters of the Muszynska seal model ($n_1 = 2, n_2 = 0.15$).

radial stiffness, damping and inertia effects respectively. The $\tau\omega D$ term in the first matrix on the right-hand side of equation (1) is the cross-stiffness, which is the most important component affecting the rotor instability.

According to both experiments and numerical simulations [6, 15], K , D and τ are the non-linear functions of the rotor eccentricity, which can be expressed as

$$K = K_0(1 - e)^{-n_1}, \quad D = D_0(1 - e)^{-n_1}, \quad n_1 = \frac{1}{2}, 1, \frac{3}{2}, \dots, 3, \quad \tau = \tau_0(1 - e)^{n_2},$$

$$0 < n_2 < 1.$$

where $e = |z|/c$, $z = x + iy$, $i = \sqrt{-1}$ and c is the radial clearance of the seal. The expressions of K , D are given in reference [5], while τ is suggested by the authors based on the graphic presentation in reference [5]. The n_1 and n_2 values depend on the seal considered. Figure 1 shows typical plots of K , D and τ . Let the eccentricity ratio $e = 0$ in the above functions, then the fluid dynamic forces described by equation (1) are linear and the terms in three 2×2 matrices are usually referred to as dynamic coefficients [2, 3], which are generally effective for $e \leq 0.5$. τ_0 is near, but less than, 0.5 due to the influence of axial flow, secondary flow, and friction losses. K_0 , D_0 and m_f can be calculated using methods such as Childs' formulas of dynamic coefficients of turbulent annular seals based on Hirs' lubrication equation [2].

Consider a symmetric Jeffcott rotor mounted at both rigid ends. The seal fluid force is assumed to be acting on the disk of the shaft, as shown in Figure 2. The equations of motion of the rotor are

$$\begin{aligned} \begin{bmatrix} m & 0 \\ 0 & m \end{bmatrix} \begin{bmatrix} \ddot{\bar{x}} \\ \ddot{\bar{y}} \end{bmatrix} + \begin{bmatrix} D_e & 0 \\ 0 & D_e \end{bmatrix} \begin{bmatrix} \dot{\bar{x}} \\ \dot{\bar{y}} \end{bmatrix} + \begin{bmatrix} K_e & 0 \\ 0 & K_e \end{bmatrix} \begin{bmatrix} \bar{x} \\ \bar{y} \end{bmatrix} \\ = \begin{bmatrix} F_x \\ F_y \end{bmatrix} + \begin{bmatrix} 0 \\ -mg \end{bmatrix} + mr_0\omega^2 \begin{bmatrix} \cos \omega t \\ \sin \omega t \end{bmatrix}. \end{aligned} \quad (2)$$

where m and r_0 are the mass and radius of imbalance of the disk and K_e , D_e the stiffness and external damping coefficients respectively. By introducing the following dimensionless variables: $\bar{x} = x/c$, $\bar{y} = y/c$, $\bar{t} = \omega t$, the dimensionless equations of the rotor/seal system may be rewritten by combining equations (1) and (2) such that (dropping all overbars for

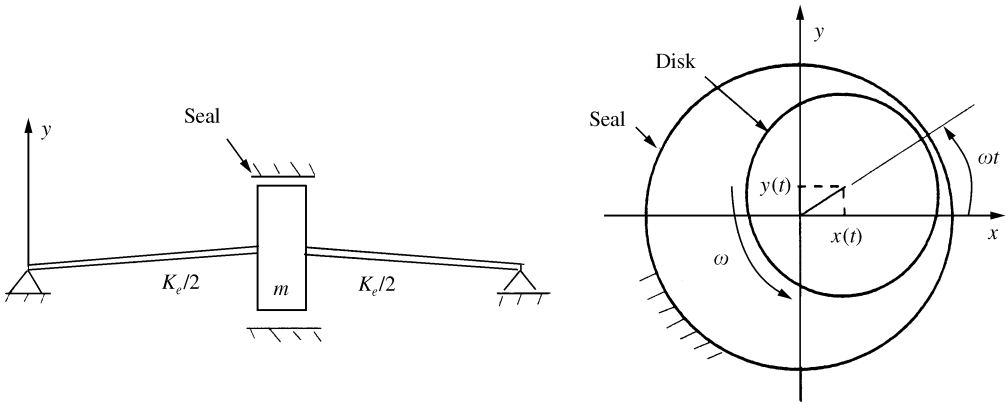


Figure 2. Rotor/seal model.

convenience)

$$\begin{bmatrix} 1 & 0 \\ 0 & 1 \end{bmatrix} \begin{bmatrix} \ddot{x} \\ \ddot{y} \end{bmatrix} + \begin{bmatrix} D_1 & D_2 \\ -D_2 & D_1 \end{bmatrix} \begin{bmatrix} \dot{x} \\ \dot{y} \end{bmatrix} + \begin{bmatrix} K_1 & K_2 \\ -K_2 & K_1 \end{bmatrix} \begin{bmatrix} x \\ y \end{bmatrix} = \begin{bmatrix} 0 \\ G \end{bmatrix} + \rho^2 \begin{bmatrix} \cos t \\ \sin t \end{bmatrix}. \quad (3)$$

where

$$K_1 = (K_e + K - \tau^2 \omega^2 m_f) / M \omega^2, \quad K_2 = \tau D / M \omega, \quad D_1 = (D_e + D) / M \omega, \\ D_2 = 2\tau m_f / M, \quad G = -mg / M c \omega^2, \quad M = m + m_f, \quad \rho^2 = m r_0 / M c.$$

3. HOPF BIFURCATION OF THE BALANCED SYSTEM

3.1. EQUILIBRIUM POSITION AND STABILITY

The static equilibrium position of the perfectly balanced rotor (i.e., $\rho = 0$ in equation (3)), $(x, \dot{x}, y, \dot{y})_0 = (x_0, 0, y_0, 0)$, which depends on the rotating speed ω , can be obtained by setting all derivative terms in equations (3) to be zero, thus

$$K_1 x_0 + K_2 y_0 = 0, \quad -K_2 x_0 + K_1 y_0 = G. \quad (4)$$

Letting $\mathbf{X} = (x - x_0, \dot{x}, y - y_0, \dot{y})^T$, one performs a Taylor-series expansion of equation (3) about the static equilibrium position $(x_0, 0, y_0, 0)$, which yields the perturbation equations

$$\mathbf{X} = \mathbf{A}(\omega)\mathbf{X} + \mathbf{F}(\omega, X), \quad (5)$$

where

$$\mathbf{A}(\omega) = -\frac{1}{M} \begin{bmatrix} 0 & -M & 0 & 0 \\ a_1 & a_2 & a_3 & a_4 \\ 0 & 0 & 0 & -M \\ b_1 & b_2 & b_3 & b_4 \end{bmatrix}, \quad \mathbf{F}(\omega, X) = -\frac{1}{M} \begin{bmatrix} 0 \\ f_{1N} \\ 0 \\ f_{2N} \end{bmatrix},$$

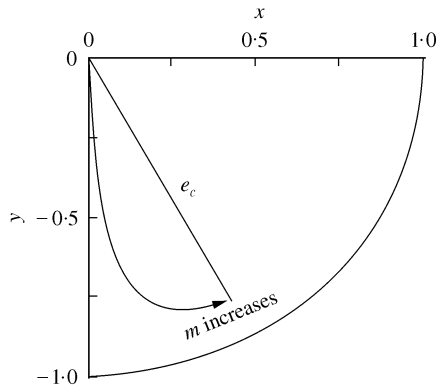


Figure 3. Stability chart.

the eight coefficients a_j, b_j ($j = 1, 2, 3, 4$) in $\mathbf{A}(\omega)$ are functions of x_0, y_0 (Appendix C), while f_{1N} and f_{2N} are higher order terms of the expansion. Obviously, $X = 0$ is the static equilibrium position of equation (5).

The eigenvalues of the matrix $A(\omega)$ satisfy the characteristic equation

$$\lambda^4 + a\lambda^3 + b\lambda^2 + c\lambda + d = 0, \quad (6)$$

where

$$a = (1/M)(a_2 + a_4), \quad b = (1/M^2)(a_2b_4 - a_4b_2) + (1/M)(a_1 + b_3),$$

$$c = (1/M^2)(a_1b_4 + a_2b_3 - a_3b_2 - a_4b_1), \quad d = 1/M^2(a_1b_3 - a_3b_1).$$

Then the stability of $X = 0$ is determined by the roots of equation (6). Due to $a = 2(D_e + D)/(M\omega) > 0$, a pair of pure imaginary roots $\lambda_{1,2} = \pm i\Omega_c = \pm i\sqrt{c/a}$ can be obtained from equation (6) when the conditions

$$(c/a)(c/a - b) + d = 0, \quad c/a - b < 0, \quad c > 0. \quad (7)$$

are satisfied whilst the other two roots of equation (6) have negative real parts: $\lambda_{3,4} = -\sigma_1 \pm i\sigma_2$, $\sigma_1 > 0$. By Routh's criterion, the rotor will lose its stability when $\omega \geq \omega_c$, where ω_c is the solution of the first equation of equation (7) and defined as the threshold speed. In other words, when the threshold speed is exceeded, the rotor/seal system becomes unstable.

Suppose $m_f = 0$ (for $m_f \ll m$), one gets the threshold speed and the dimensionless whirl frequency (the ratio of whirl speed to the threshold speed):

$$\omega_c = \frac{1}{\sqrt{\tau(\tau + e_c\tau')}} \sqrt{\left(1 + \frac{D_c}{D}\right)^2 \frac{2K_c + 2K + K'e_c}{2M} + \left(\frac{K'e_c}{2D}\right)^2}.$$

$$\Omega_c = \sqrt{c/a} = (1/\omega_c) \sqrt{(K_c + K + K'e_c)/M}. \quad (8)$$

where $(\prime) = \partial(\)/\partial e_c$. e_c is known as the critical eccentricity ratio and has relationship with mass m as shown in Figure 3. Detailed values can also be found in Table 1. ω_c and Ω_c are calculated as functions of e_c as shown in Figure 4. As mentioned above, the instability of the

TABLE 1
Results of Hopf bifurcation from Poore's criterion

$m(\text{kg})$	e_c	$\alpha'(0) \times 10^3$	$\delta'(0)$	$\text{Re } c_1(0) \times 10^3$	$\text{Im } c_1(0) \times 10^3$
2000	0.19	0.026	0.049	-0.01	-0.01
3000	0.29	0.034	0.074	-0.03	-0.02
4000	0.38	0.050	0.160	-0.08	-0.04
5000	0.47	0.069	0.475	-0.33	-0.12
6000	0.56	0.100	1.274	-1.27	-0.35
7000	0.64	0.134	3.067	-4.12	-0.05
8000	0.71	0.168	3.883	-6.53	1.28
9000	0.77	0.196	2.931	-5.74	1.93
10000	0.81	0.217	2.235	-4.86	1.83
11000	0.83	0.225	1.875	-4.22	1.68

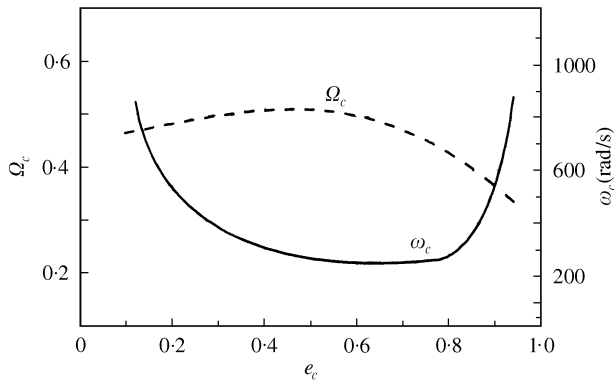


Figure 4. The relationship between the critical eccentricity and mass.

rotor/seal system is mainly affected by the cross stiffness $\tau\omega D$. Because there is difference between the ascending rate of D and descending rate of τ as the rotor's eccentricity is increased, the change of the threshold speed ω_c with e_c can either increase or decrease. The minimum occurs when $e_c = 0.6-0.75$. When e_c exceeds 0.8, ω_c increases very rapidly, which means that the occurrence of instability in heavy rotors is rare (similar to rotor/bearing systems, the rotor is always stable for $e_c > 0.8$ [10]). Ω_c is near 0.5 for a large range of values of e_c but decreases as e_c gets larger than 0.8. This behaviour reflects the decrease of the average circumferential velocity of the fluid inside the seal.

3.2. HOPF BIFURCATION AND NUMERICAL SIMULATION

Let $\sigma = \omega - \omega_c$ be a small parameter, which measures the deviation of ω away from ω_c . So $(X, \sigma) = (0, 0)$ is the critical static equilibrium position of equation (5). The eigenvalues of $A(\omega_c + \sigma)$ are $\lambda_{1,2} = \alpha(\sigma) \pm i\Omega(\sigma)$ and $\lambda_{3,4} = -\sigma_1(\sigma) \pm i\sigma_2(\sigma)$ with $\alpha(0) = 0$, $\Omega(0) = \Omega_c$ and $\sigma_1(0) > 0$. Table 1 indicates that $\alpha'(0) = (d\alpha/d\omega)_{\sigma=0} > 0$ in the displayed range of value of e_c . Therefore, the conditions of the Hopf bifurcation are satisfied (Appendix A). The direction of bifurcation and the stability of the bifurcated periodic orbit can be determined using

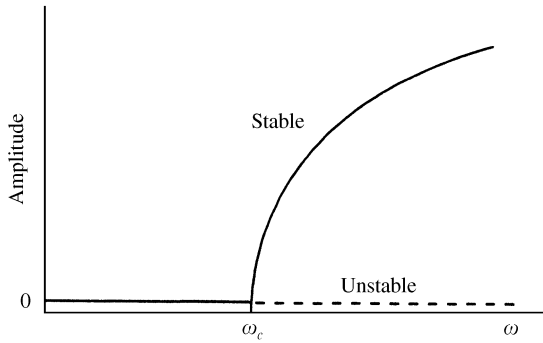


Figure 5. Supercritical Hopf bifurcation.

Poore's algebraic formulas (Appendix B). From Table 1 one sees that supercritical bifurcation will take place for $\sigma > 0$ due to $\delta'(0) > 0$ and $\alpha'(0) > 0$, and it means that the small-amplitude periodic whirl with dimensionless frequency Ω_c exists when the threshold speed ω_c is exceeded (Figure 5). Such a motion is often referred to as lower-frequency self-excited vibration for $\Omega_c < 1$ indicating the whirl speed is lower than the rotor's rotating speed.

To verify the theoretical results, a numerical investigation using the Runge-Kutta algorithm was carried out. Taking $m = 3000$ kg, one finds that the eccentricity $e_c = 0.29$ and $\omega_c = 371$ rad/s (from Table 1 and Figure 4). The transient motion of the rotor at different speeds and initial conditions are shown in Figure 6 in which the initial speeds in two directions are always set as zero. Figure 6(a) illustrates the static equilibrium position (left) and the transient motion starting from two positions (right) when $\omega = 365$ rad/s. Below the threshold speed, the rotor is stable and spirals into the equilibrium position in dependent of the initial condition. Above the threshold speed, a stable whirl orbit, also independent of the initial conditions, should appear according to the Hopf bifurcation theory. The numerical results support the theoretical prediction, as shown in Figure 6(b-d). The initial conditions are chosen to be either close to the critical static equilibrium position $(0, -0.2)$ and also far from it $(1, 0)$. Both conditions result in identical final whirl orbits for the same speed. So the whirl orbit is stable. The amplitude of the stable orbit increases steadily as the rotor speed is increased. Eventually, the increase of the orbit amplitude will result in rubbing between the rotor and seal, at well above its threshold speed, due to loss of ability of bearing the weight by the fluid inside the seal. In this case the seal fluid force model is invalid [5].

4. PERIODICALLY PERTURBED HOPF BIFURCATION IN $\frac{1}{2}$ SUBHARMONIC RESONANCE OF THE IMBALANCED SYSTEM

4.1. REDUCTION AND AVERAGING

For the imbalanced system (i.e., $\rho \neq 0$ in equation (3)), the perturbation equations about the static equilibrium position $(\cdot)_0$ determined in equation (4) are deduced as

$$\mathbf{X} = \mathbf{A}(\omega)\mathbf{X} + \mathbf{F}(\omega, X) + \rho^2\mathbf{\Gamma}(t), \quad (9)$$

where $\rho^2\mathbf{\Gamma}(t) = \rho^2 (0, \cos t, 0, \sin t)^T$ is a periodic perturbation term. Generally, the imbalance ρ is of small level, which leads to a periodical perturbation to the Hopf

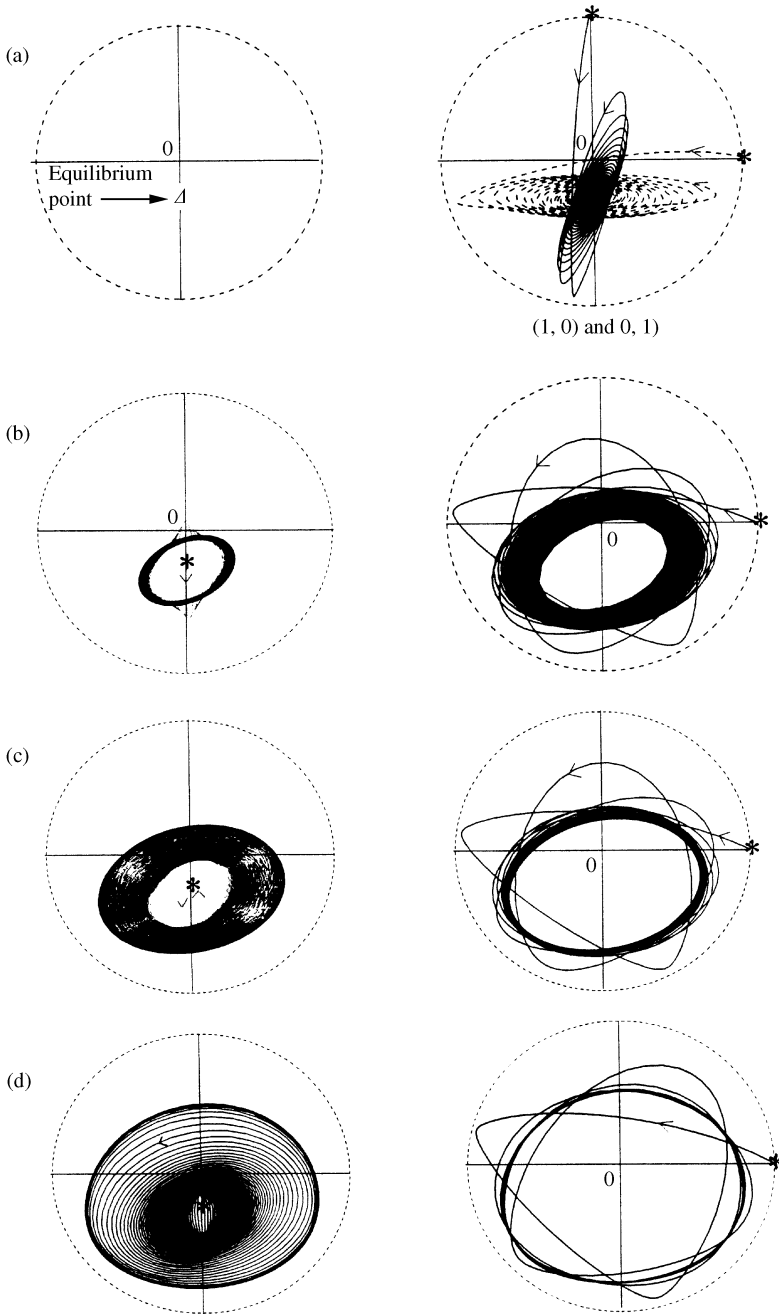


Figure 6. Whirl orbit of the rotor in different speeds and from different initial positions (indicated by *): (a) $\omega = 365$ 1/s; (b) $\omega = 380$ 1/s; (c) $\omega = 400$ 1/s; (d) $\omega = 460$ 1/s.

bifurcation of the system when operating in the neighbourhood of the threshold speed ω_c . Due to the dimensionless whirl frequencies Ω_c being close to $\frac{1}{2}$ over quite a large range of the system parameters, there exists a possibility of a subharmonic resonance of order 2 for the bifurcation motion (non-synchronized whirl).

Letting $\omega = \omega_c + \sigma$ and expanding A and F in equations (9) up to order 1 of σ , one gets

$$\dot{\mathbf{X}} = \mathbf{A}_c \mathbf{X} + \sigma \bar{\mathbf{A}}(\omega_c) \mathbf{X} + \mathbf{F}(\omega_c, X) + \sigma \bar{\mathbf{F}}(\omega_c, X) + \rho^2 \mathbf{\Gamma}(t). \tag{10}$$

where $\mathbf{A}_c = \mathbf{A}(\omega_c)$ with eigenvalues of $\pm i\Omega_c$ and $-\sigma_1 \pm i\sigma_2, \sigma_1 > 0$. Introducing the co-ordinate transformation $\mathbf{X} = \mathbf{Q}\mathbf{Y}$, $\mathbf{Y} = (y_1, y_2, y_3, y_4)^T$, where $\mathbf{Q} = [Q_{ij}]_{4 \times 4}$ contains the eigenvectors corresponding to the eigenvalues of \mathbf{A}_c , and treating $t \pmod{2\pi}$, σ, ρ as dependent variables, equation (10) yields

$$\dot{t} = 1, \quad \dot{\rho} = 0, \quad \dot{\sigma} = 0,$$

$$\begin{aligned} \begin{bmatrix} \dot{y}_1 \\ \dot{y}_2 \end{bmatrix} &= \mathbf{B}_0 \begin{bmatrix} y_1 \\ y_2 \end{bmatrix} + \sigma \mathbf{B}_1 \begin{bmatrix} y_1 \\ y_2 \end{bmatrix} + \sigma \mathbf{B}_2 \begin{bmatrix} y_3 \\ y_4 \end{bmatrix} + \mathbf{B}_3(Y) + \sigma \mathbf{B}_4(Y) + \rho^2 \mathbf{B}_5 \begin{bmatrix} \cos t \\ \sin t \end{bmatrix}, \\ \begin{bmatrix} \dot{y}_3 \\ \dot{y}_4 \end{bmatrix} &= \mathbf{C}_0 \begin{bmatrix} y_3 \\ y_4 \end{bmatrix} + \sigma \mathbf{C}_1 \begin{bmatrix} y_1 \\ y_2 \end{bmatrix} + \sigma \mathbf{C}_2 \begin{bmatrix} y_3 \\ y_4 \end{bmatrix} + \mathbf{C}_3(Y) + \sigma \mathbf{C}_4(Y) + \rho^2 \mathbf{C}_5 \begin{bmatrix} \cos t \\ \sin t \end{bmatrix}, \end{aligned} \tag{11}$$

where

$$\mathbf{B}_0 = \begin{bmatrix} 0 & \Omega_c \\ -\Omega_c & 0 \end{bmatrix}, \quad \mathbf{C}_0 = \begin{bmatrix} -\sigma_1 & \sigma_2 \\ -\sigma_2 & -\sigma_1 \end{bmatrix}.$$

\mathbf{B}_i and \mathbf{C}_i ($j = 1, 2, 5$) are constant (2×2) matrices, $\mathbf{B}_i(Y)$ and $\mathbf{C}_i(Y)$ ($j = 3, 4$) are (2×1) matrices with non-linear polynomials.

According to centre manifold theory [16], the two-dimensional centre manifold $\mathbf{H} = (h_1, h_2)^T$ exists and can be expressed as

$$\begin{aligned} \mathbf{H} = \begin{bmatrix} y_3 \\ y_4 \end{bmatrix} &= \begin{bmatrix} h_1(y_1, y_2, \sigma, \rho, t) \\ h_2(y_1, y_2, \sigma, \rho, t) \end{bmatrix} = \begin{bmatrix} d_1 \\ e_1 \end{bmatrix} y_1^2 + \begin{bmatrix} d_2 \\ e_2 \end{bmatrix} y_1 y_2 + \begin{bmatrix} d_3 \\ e_3 \end{bmatrix} y_2^2 \\ &+ \begin{bmatrix} d_4 \\ e_4 \end{bmatrix} \sigma y_1 + \begin{bmatrix} d_5 \\ e_5 \end{bmatrix} \sigma y_2 + \begin{bmatrix} d_6 \\ e_6 \end{bmatrix} \rho^2 \sin t + \begin{bmatrix} d_7 \\ e_7 \end{bmatrix} \rho^2 \cos t. \end{aligned} \tag{12}$$

Obviously, $\mathbf{H}(\underline{0}) = \mathbf{D}_y \mathbf{H}(\underline{0}) = 0$, where $(\underline{0})$ means $\sigma = \rho = y_1 = y_2 = 0$, and $\mathbf{D}_y \mathbf{H}$ is the Frechet derivative of h

$$\mathbf{D}_y \mathbf{H} = \begin{bmatrix} \partial h_1 / \partial y_1 & \partial h_1 / \partial y_2 \\ \partial h_2 / \partial y_1 & \partial h_2 / \partial y_2 \end{bmatrix}.$$

$\rho^2 \sin t$ and $\rho^2 \cos t$ represent the forced vibration induced by the mass imbalance of the disk.

Taking the derivative of equation (12), and considering equation (11), one gets the equations

$$\begin{aligned} N(H) = \mathbf{D}_y \mathbf{H} \left\{ \mathbf{B}_0 \begin{bmatrix} y_1 \\ y_2 \end{bmatrix} + \sigma \mathbf{B}_1 \begin{bmatrix} y_1 \\ y_2 \end{bmatrix} + \sigma \mathbf{B}_2 \begin{bmatrix} h_1 \\ h_2 \end{bmatrix} + \mathbf{B}_3(y_1, y_2) + \sigma \mathbf{B}_4(y_1, y_2) \right. \\ \left. + \rho^2 \mathbf{B}_5 \begin{bmatrix} \cos t \\ \sin t \end{bmatrix} \right\} + \rho^2 \begin{bmatrix} d_6 & -d_7 \\ e_6 & -e_7 \end{bmatrix} \begin{bmatrix} \cos t \\ \sin t \end{bmatrix} - \left\{ \mathbf{C}_0 \begin{bmatrix} h_1 \\ h_2 \end{bmatrix} + \sigma \mathbf{C}_1 \begin{bmatrix} y_1 \\ y_2 \end{bmatrix} \right. \\ \left. + \sigma \mathbf{C}_2 \begin{bmatrix} h_1 \\ h_2 \end{bmatrix} + \mathbf{C}_3(y_1, y_2) + \sigma \mathbf{C}_4(y_1, y_2) + \rho^2 \mathbf{C}_5 \begin{bmatrix} \cos t \\ \sin t \end{bmatrix} \right\} = 0. \end{aligned}$$

The condition for obtaining approximated \mathbf{H} up to order 2 can be deduced from the above equation as

$$\begin{aligned}
 &D_y \mathbf{H} \cdot \mathbf{B}_0 \begin{bmatrix} y_1 \\ y_2 \end{bmatrix} - \mathbf{C}_0 \begin{bmatrix} h_1 \\ h_2 \end{bmatrix} - \sigma \mathbf{C}_1 \begin{bmatrix} y_1 \\ y_2 \end{bmatrix} - \mathbf{C}_3^{(2)}(y_1, y_2) - \rho^2 \mathbf{C}_5 \begin{bmatrix} \cos t \\ \sin t \end{bmatrix} \\
 &+ \rho^2 \begin{bmatrix} d_6 & -d_7 \\ e_6 & -e_7 \end{bmatrix} \begin{bmatrix} \cos t \\ \sin t \end{bmatrix} = 0.
 \end{aligned} \tag{13}$$

where $\mathbf{C}_3^{(2)}(y_1, y_2)$ represents the quadratic terms in $\mathbf{C}_3(y_1, y_2)$. The coefficients d_i and $e_i (j = 1-7)$ in equation (12) can be obtained by solving equation (13). Substituting the determined \mathbf{H} into equation (11), one gets the governing equations of dynamics on the centre manifold (after transforming the linear parts into Jordan canonical form)

$$\begin{aligned}
 \begin{bmatrix} \dot{u}_1 \\ \dot{u}_2 \end{bmatrix} &= \begin{bmatrix} \alpha(\sigma) & \Omega(\sigma) \\ -\Omega(\sigma) & \alpha(\sigma) \end{bmatrix} \begin{bmatrix} u_1 \\ u_2 \end{bmatrix} + \rho^2 \begin{bmatrix} H_1(u, t) \\ H_2(u, t) \end{bmatrix} + \begin{bmatrix} N_1^{(2)}(u, \sigma) \\ N_2^{(2)}(u, \sigma) \end{bmatrix} + \begin{bmatrix} N_1^{(3)}(u, \sigma) \\ N_2^{(3)}(u, \sigma) \end{bmatrix} \\
 &+ \rho^2 \bar{B} \begin{bmatrix} \cos t \\ \sin t \end{bmatrix},
 \end{aligned} \tag{14}$$

where $H_j (j = 1, 2)$ is a linear polynomial of u_1 and u_2 with coefficients being the functions of t with period 2π , which represents the effects of the imbalance on the Hopf bifurcation (non-synchronized whirl) of the rotor through parametric excitation. $N_j^{(2)}$ and $N_j^{(3)}$ are quadratic and cubic polynomials of u_1 and u_2 with $N_j^{(2)}(u, 0) \neq 0$ and $N_j^{(3)}(u, 0) \neq 0$, respectively, and \bar{B} is a constant 2×2 matrix.

For the study of subharmonic resonance of order 2, we have $\Omega_c = 1/2 + \varepsilon\mu$, where ε is a positive small parameter and μ a detuning parameter. $\varepsilon\mu$ measures the deviation of Ω_c away from $\frac{1}{2}$. Letting $\sigma = \varepsilon\bar{\sigma}$, $\rho^2 = \varepsilon\bar{\rho}$, one gets $\alpha(\sigma) = \alpha'(0)\sigma + O(\sigma^2) = \varepsilon\alpha'(0)\bar{\sigma} + O(\varepsilon^2)$, $\Omega(\sigma) = \Omega_c + \Omega'(0)\sigma + O(\sigma^2) = 1/2 + \varepsilon(\Omega'(0)\bar{\sigma} + \mu) + O(\varepsilon^2)$. Rescaling the state vector $(u_1, u_2)^T$ in equation (14) by the transformation $(u_1, u_2)^T = \varepsilon^{1/2}(v_1, v_2)^T$, then transform the obtained equations from v_1, v_2 to new variables r, φ , the amplitude and the phase of the solution respectively, the means of the transformation.

$$v_1 = r \cos \theta, \quad v_2 = r \sin \theta, \quad \theta = \frac{1}{2}t + \varphi.$$

a set of equations in standard form, up to $O(\varepsilon)$, is obtained (dropping all overbars for convenience) as

$$\dot{r} = \varepsilon\alpha'(0)\sigma r + \varepsilon^{1/2}\rho r H'(\varphi, t, 1/2) + \varepsilon^{1/2} N_1'(r, \theta) + \varepsilon N_2'(r, \theta) + \varepsilon^{1/2}\rho B'(t).$$

$$r\dot{\varphi} = \varepsilon r [\mu + \Omega'(0)\sigma] + \varepsilon^{1/2}\rho r H''(\varphi, t, 1/2) + \varepsilon^{1/2} N_1''(r, \theta) + \varepsilon N_2''(r, \theta) + \varepsilon^{1/2}\rho B''(t). \tag{15}$$

where H' and H'' contain constant terms (including φ) and periodic terms with period 2π , B' and B'' periodic terms only and N_j', N_j'' quadratic and cubic polynomials of r respectively. The averaged equations in subharmonic resonance of order 2 can be obtained by applying the averaging operator among a period 2π to the right side of equations (15) to the second approximation (in order to include the influence of quadratic non-linear terms) as

$$\begin{aligned}
 \dot{r} &= \varepsilon [\alpha'(0)\sigma r + \text{Re } c_1 \frac{1}{2}, \sigma) r^3 + r\rho U \sin 2(\varphi + \beta)]. \\
 r\dot{\varphi} &= \varepsilon r [\Omega'(0)\sigma + \mu + \text{Im } c_1 \frac{1}{2}, \sigma) r^2 + \rho U \cos 2(\varphi + \beta)].
 \end{aligned} \tag{16}$$

where $U (>0)$ and β are constants. $\text{Re } c_1(\frac{1}{2}, \sigma)$ and $\text{Im } c_1(\frac{1}{2}, \sigma)$, resulting from the non-linear autonomous terms in equation (15), are equal to $\text{Re } c_1(\gamma)$ and $\text{Im } c_1(\gamma)$ in equations (A3) (Appendix A), respectively, due to the equivalence of the averaging method and normal form method [17]. By expansion up to order 1 of σ , one gets

$$\text{Re } c_1(1/2, \sigma) = \text{Re } c_1(1/2, 0) + O(\sigma), \quad \text{Im } c_1(1/2, \sigma) = \text{Im } c_1(1/2, 0) + O(\sigma).$$

where $\text{Re } c_1(1/2, 0)$ and $\text{Im } c_1(1/2, 0)$ have been obtained by Poore's criteria (Table 1).

4.2. STABILITY AND BIFURCATION OF THE AVERAGED SYSTEM

The stationary responses of the averaged equations (16) are determined by setting $\dot{r} = \dot{\phi} = 0$, which yields (from the leading order terms)

$$A_1 r^4 + A_2 r^2 + A_3 = 0, \quad r = 0, \quad (17, 18)$$

where

$$\begin{aligned} A_1 &= R^2 + I^2, & A_2 &= 2[R\Omega'(0) + I\Omega'(0)]\sigma + \mu, \\ A_3 &= (\alpha'(0)\sigma)^2 + (\Omega'(0)\sigma + \mu)^2 - (\rho U)^2, & R &= \text{Re } c_1(1/2, 0), & I &= \text{Im } c_1(1/2, 0). \end{aligned}$$

The non-trivial solutions of equation (17) are

$$r_{1,2} = (-A_2 \pm \sqrt{\Delta})^{1/2} / \sqrt{2A_1}. \quad (19)$$

where

$$\Delta = A_2^2 - 4A_1A_3 = 4\{-[R\Omega'(0) - I\alpha'(0)]\sigma + R\mu\}^2 + A_1(\rho U)^2\}.$$

By examining the non-trivial solutions of equation (19), equation (17) has

(1) one positive real root r_1 provided $A_3 < 0$

$$(\alpha'(0)\sigma)^2 + (\Omega'(0)\sigma + \mu)^2 < (\rho U)^2, \quad (20)$$

(2) two positive real root r_1, r_2 provided $A_2 < 0$, $-4A_1A_3 \leq 0$ and $\Delta \geq 0$:

$$\begin{aligned} [R\alpha'(0) + I\Omega'(0)]\sigma + I\mu &< 0, & (\alpha'(0)\sigma)^2 + (\Omega'(0)\sigma + \mu)^2 &\geq (\rho U)^2, \\ A_1 U^2 \rho^2 &\geq [(R\Omega'(0) - I\alpha'(0)]\sigma + R\mu]^2. \end{aligned} \quad (21)$$

4.2.1. Stability of the trivial solution

Introducing $z_1 = r \cos(\phi + \beta)$, $z_2 = r \sin(\phi + \beta)$, equation (16) can be transformed as

$$\begin{aligned} \dot{z}_1 &= \varepsilon[\alpha'(0)\sigma z_1 + (\rho U - \Omega'(0)\sigma - \mu)z_2 + (z_1^2 + z_2^2)(Rz_1 - Iz_2)], \\ \dot{z}_2 &= \varepsilon[\rho U + \Omega'(0)\sigma + \mu]z_1 + \alpha'(0)\sigma z_2 + (z_1^2 + z_2^2)(Rz_2 - Iz_1). \end{aligned} \quad (22)$$

The linear parts of equation (22) correspond to the linear variational equations about the trivial solution, $r = 0$, and the corresponding characteristic equation is

$$\lambda^2 - 2\alpha'(0)\sigma\lambda + (\alpha'(0)\sigma)^2 + (\Omega'(0)\sigma + \mu)^2 - (\rho U)^2 = 0. \quad (23)$$

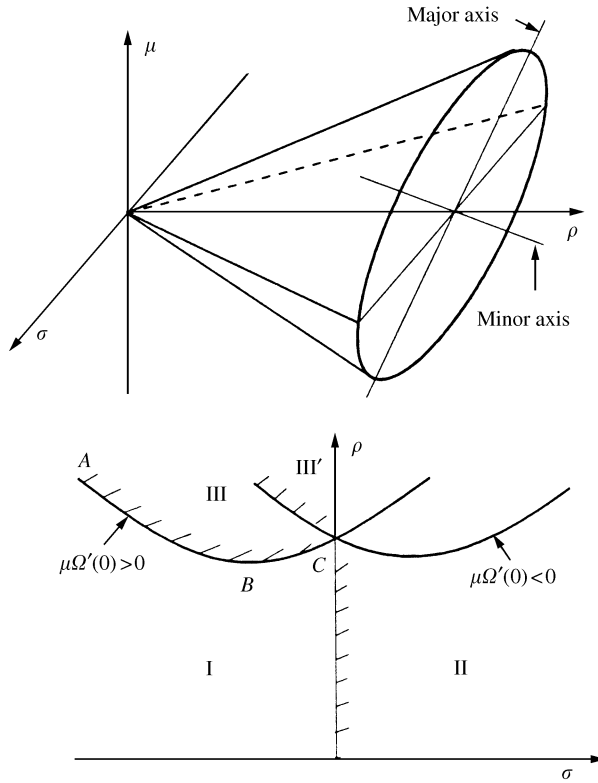


Figure 7. Stability boundary of the trivial solutions of equation (16) ($\Omega'(0) > 0$).

The trivial solution is stable if the following conditions hold ($\alpha'(0) > 0$ from Table 1):

$$\sigma < 0, \quad (\alpha'(0)\sigma)^2 + \Omega'(0)\sigma + \mu^2 > (\rho U)^2. \tag{24}$$

The second equation of equation (24) indicates the region outside the elliptic cone shown in Figure 7 (if $\Omega'(0) < 0$, one should only replace σ by $-\sigma$). Fixing μ , one gets the stability boundary for trivial solution in the (σ, ρ) plane as shown in Figure 7. There are two important points in the plane, namely

$$B: \sigma = -\frac{\mu\Omega'(0)}{(\alpha'(0))^2 + (\Omega'(0))^2}, \quad \rho = \frac{|\mu\alpha'(0)|}{U\sqrt{(\alpha'(0))^2 + \Omega'(0))^2}, \quad C: \sigma = 0, \quad \rho = |\mu|/U,$$

obviously, $\rho_C > \rho_B$. In region I, the trivial solution is stable. There are three ways for the trivial solution to lose its stability, depending on the solution of the characteristic equation (23):

- (1) Along \overline{OC} , a Hopf bifurcation (a pair of pure imaginary eigenvalues);
- (2) along \overline{BC} , a pitch-fork bifurcation (a single zero eigenvalue);
- (3) at point C, a global bifurcation (two zero eigenvalues).

The stability analysis of non-trivial solution indicates that r_2 is always unstable. r_1 is stable but will exhibit Hopf bifurcation (secondary bifurcation) at a critical value of σ under some conditions. A saddle-type bifurcation happens along $\Delta = 0$ where r_1 and r_2 coalesce.

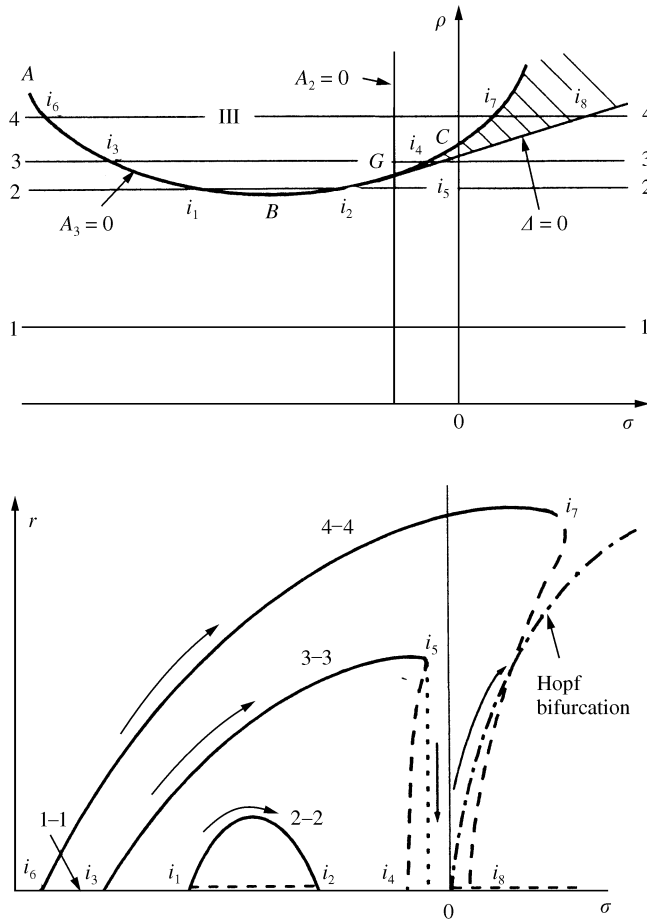


Figure 8. Bifurcation of equation (16): —, stable solutions; ---, unstable solution.

4.2.2. Bifurcation of the averaged response

From equations (20), (21) and (24), a real solution and two real solutions of the equation (17) exist in instability region III and the shaded region of Figure 8 respectively (G is the intersection point of three margin lines: $A_2 = 0$, $A_3 = 0$ and $\Delta = 0$). The occurrence of non-trivial solutions of the bifurcation equation (17) means a non-synchronized whirl to the imbalanced system. Two paths for the occurrence of bifurcation as σ is increased, for various levels of ρ , are presented in Figure 8.

- (1) Along line 1-1, the trivial solution loses its stability through Hopf bifurcation at $\sigma = 0$. For the original unbalanced system (2), the bifurcation results in a quasi-periodic motion in which the ratio of the whirling frequency to the rotating frequency is incommensurable.
- (2) Along lines 2-2, 3-3 and 4-4, the points labelled i_1, i_2, \dots, i_8 in Figure 8(b) correspond to those in Figure 8(a). The occurrence of non-trivial solution of the averaged equation (16) results in a period-doubling motion in which the above ratio is strictly $\frac{1}{2}$, known as "half-frequency whirl", to the original imbalanced system. It should be noted that σ is less than 0 when it arrives at AB, i.e., $\omega < \omega_c$, which means the

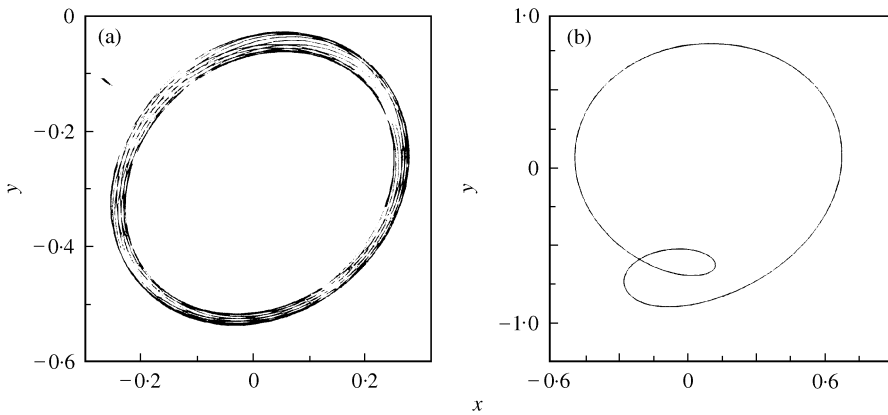


Figure 9. Orbits of non-synchronized motion of the rotor/seal system: (a) quasi-periodic motion ($r_0 = 0.1$ mm, $\omega = 378$ rad/s $> \omega_c$); (b) period-doubling motion ($r_0 = 0.4$ mm) $\omega = 355$ rad/s $< \omega_c$).

period-doubling bifurcation occurs before the threshold speed determined by linear model is exceeded. From Figure 7, one also finds that the bifurcation occurs earlier as ρ is increased, or $|\mu|$ decreased. This suggests two ways to delay or avoid the occurrence of this type of bifurcation (the instability for the normal motion) in the actual working range: (1) balancing the rotor carefully to decrease the level of the imbalance; (2) designing the parameters of the rotor system to Ω_c cause to be as far way from $\frac{1}{2}$ as possible (i.e., increase $|\mu|$).

Taking $m = 3000$ kg, one finds from Table 1 and Figure 4 that $\omega_c = 371$ rad/s and $\Omega_c \approx 0.495$. The Runge-Kutta algorithm was used to simulate the motion of the imbalanced system (2). For $r_0 = 0.1$ mm, the motion of the system is always periodic before the rotor speed exceeds its threshold value and then quasi-periodic motion is found as shown in Figure 9(a) when $\omega = 378$ rad/s ($> \omega_c$). For $r_0 = 0.4$ mm, the period-doubling motion is found before the threshold speed is exceeded as shown in Figure 9(b) when $\omega = 355$ rad/s ($< \omega_c$).

5. CONCLUSIONS

The bifurcation behaviour of a symmetric rotor/seal system has been investigated in this paper. For the balanced system, the instability from certain critical equilibrium positions was proved to be the result of Hopf bifurcation. Only supercritical bifurcation has been found for the specific rotor system using Poore's algebraic criteria. So a stable periodic orbit bifurcates from the critical steady state position. The amplitude of the whirling orbit increases gradually as the rotor speed is increased and the dimensionless whirl frequency was found to be close to $\frac{1}{2}$ over quite a large range of the system parameters. The study on the $\frac{1}{2}$ subharmonic resonance in the neighbourhood of the threshold speed for the imbalanced system shows that the non-synchronized whirl can either be a quasi-periodic motion resulting from Hopf bifurcation, or a half-frequency whirl from period-doubling bifurcation. The level of imbalance, the deviation of the dimensionless whirl frequency away from $\frac{1}{2}$ and the rotating speed of the rotor determine which one can be the actual response of the system.

REFERENCES

1. S. T. NOAH and P. SUNDARARAJAN 1995 *Journal of Vibration and Control* **1**, 431–458. Significance of considering nonlinear effects in predicting the dynamic behavior of rotating machinery.
2. D. W. CHILDS 1983 *Transaction of American Society of Mechanical Engineers, Journal of Lubrication Technology* **105**, 429–436. Dynamic analysis of turbulent annular seals based on Hirs' lubrication equation.
3. L. A. SAN ANDRES 1993 *Transaction of American Society of Mechanical Engineers, Journal of Tribology* **115**, 61–70. Dynamic force and moment coefficients for short length annular seals.
4. A. MUSZYNSKA 1986 *Journal of Sound and Vibration* **110**, 443–462. Whirl and whip-rotor/bearing stability problems.
5. A. MUSZYNSKA 1988 *Transaction of American Society of Mechanical Engineers, Journal of Vibration, Acoustics, Stress and Reliability in Design* **110**, 129–136. Improvements in lightly loaded rotor/bearing and rotor/seal models.
6. A. MUSZYNSKA and D. E. BENTLY 1990 *Journal of Sound and Vibration* **143**, 103–124. Frequency-swept rotating input perturbation techniques and identification of the fluid force models in rotor/bearing/seal systems and fluid handling machines.
7. A. MUSZYNSKA and D. E. BENTLY 1989 *Transaction of American Society of Mechanical Engineers, Journal of Vibration, Acoustics, Stress and Reliability in Design* **111**, 156–162. Anti-swirl arrangements prevent rotor/seal instability.
8. T. KAPITANIAK 1991 *Chaotic Oscillations in Mechanical Systems*. Manchester and New York: Manchester University Press.
9. A. B. POORE 1976 *Archives for Rational Mechanics and Analysis* **60**, 371–392. On the theory of an application of the Hopf bifurcation theory.
10. C. J. MYERS 1984 *Transaction of American Society of Mechanical Engineers, Journal of Applied Mechanics* **51**, 244–250. Bifurcation theory applied to oil whirl in plain cylindrical journal bearings.
11. A. K. BAJAJ 1987 *International Journal of Nonlinear Mechanics* **22**, 47–59. Bifurcation in parametrically forced nonlinear oscillator.
12. J. M. GAMBAUDO 1985 *Journal of Differential Equations* **57**, 172–199. Perturbation of a Hopf bifurcation by an external time-periodic forcing.
13. N. SRI NAMACHCHIVAYA and S. T. ARIARATNAM 1987 *SIAM Journal of Applied Mathematics* **47**, 15–39. Periodically perturbed Hopf bifurcation.
14. J. SHAW and S. SHAW 1990 *Nonlinear Dynamics* **1**, 293–311. The effects of unbalance on oil whirl.
15. L. T. TAM, A. J. PRZEKwas, A. MUSZYNSKA, R. C. HENDRICKS, M. J. BRAUN and R. L. MULLEN 1988 *Transaction of American Society of Mechanical Engineers, Journal of Vibration, Acoustics, Stress and Reliability in Design* **110**, 315–325. Numerical and analytical study of fluid dynamic forces in seals and bearings.
16. J. CARR 1981 *Application of Center Manifold Theory*. New York: Springer.
17. P. R. SETHNA 1995 *Nonlinear Dynamics* **7**, 1–10. On averaged and normal form equations.

APPENDIX A: HOPF BIFURCATION THEORY

Consider the differential equation

$$dx/dt = F(x, \gamma), \quad F: R^n \times R \rightarrow R^n, \quad n \geq 2, \quad F \in C^\infty. \quad (\text{A1})$$

where γ is a real parameter. Assume that:

- (1) $x = a^0$ is an equilibrium position of equation (A1), that is $F(a^0, 0) = 0$.
- (2) The Jacobian matrix $A(\gamma) = D_x F(a^0, \gamma)$ has a pair of eigenvalues $\alpha(\gamma) \pm i\Omega(\gamma)$ which satisfy $\alpha(0) = 0$, $\Omega(0) = \Omega_c > 0$ and $(n - 2)$ eigenvalues with non-zero real parts.
- (3) F is differentiable in a neighbourhood of $(x, \gamma) = (a^0, 0)$.
- (4) $\alpha'(0) = (d\alpha/d\gamma)|_{\gamma=0} \neq 0$, where $\alpha(\gamma) \pm i\Omega(\gamma)$ denotes that eigenvalue of $A(\gamma) = D_x F(a^0, \gamma)$ is a continuous extension of $\pm i\Omega_c$.

Under these conditions, there will be a non-constant periodic orbit bifurcating from $(x, \gamma) = (a^0, 0)$. To analyze the bifurcation solution, equation (A1) is reduced using centre

manifold procedure to the two dimension system as

$$\mathbf{y}' = \mathbf{A}(\gamma)\mathbf{y} + \mathbf{F}^{(2)}(\mathbf{y}) + \mathbf{F}^{(3)}(\mathbf{y}) + \text{h.ot.} \tag{A2}$$

where $\mathbf{y} = (y_1, y_2)^T$ is real variables, $\mathbf{F}^{(j)}(\mathbf{y})$ is the quadratic ($j = 2$) and cubic ($j = 3$) polynomials of y_1, y_2 . The Poincaré–Birkhoff normal form of equation (A2) in polar co-ordinates is

$$\begin{aligned} r' &= \alpha(\gamma)r + \sum_{j=1}^m \text{Re } c_j(\gamma)r^{2j+1} + O(r^{2m+2}), \\ \theta' &= \Omega(\gamma) + \sum_{j=1}^m \text{Im } c_j(\gamma)r^{2j} + O(r^{2m+1}). \end{aligned} \tag{A3}$$

The non-trivial solution of equation (A3) is

$$\begin{aligned} r = \varepsilon, \quad \gamma(\varepsilon) &= \gamma_2\varepsilon^2 + \gamma_4\varepsilon^4 + \dots, \quad T(\varepsilon) = (2\pi/\Omega_c)(1 + \tau_2\varepsilon^2 + \tau_4\varepsilon^4 + \dots), \\ \gamma_2 &= -\text{Re } c_1(0)/\alpha'(0), \quad \tau_2 = -(1/\Omega_c)[\Omega'(0)\gamma_2 + \text{Im } c_1(0)], \end{aligned}$$

where $T(\varepsilon)$ is the period of the solution.

APPENDIX B: POORE'S ALGEBRAIC FORMULAS

Assume the derivative $(d\alpha/d\gamma)|_{\gamma=0} \neq 0$ and the remaining $(n - 2)$ eigenvalues of $\mathbf{A}(0) = \mathbf{D}_x\mathbf{F}(a^0, 0)$ have negative real parts, the direction of bifurcation (non-degenerated) and the stability of the periodic orbit can be determined by the result of the following algebraic formula:

$$\begin{aligned} 8\alpha'(0)\delta'(0) + i8(\Omega'(0)\delta'(0) + \Omega_c\eta'(0)) &= -\mathbf{u}\mathbf{F}_{xxx}vv\bar{v} + 2\mathbf{u}\mathbf{F}_{xx}\mathbf{v}(\mathbf{A}^0)^{-1}\mathbf{F}_{xx}\mathbf{v}\bar{v} \\ &+ \mathbf{u}\mathbf{F}_{xx}\bar{\mathbf{v}}(\mathbf{A}^0 - i2\Omega_c\mathbf{I})^{-1}\mathbf{F}_{xx}\mathbf{v}\mathbf{v}. \end{aligned} \tag{B1}$$

where $\mathbf{A}^0 = \mathbf{A}(0)$; \mathbf{u} and \mathbf{v} , having been normalized by the requirement $\mathbf{u}\mathbf{v} = 1$, are the left and right eigenvectors for the eigenvalues $+i\Omega_c$ of \mathbf{A}^0 respectively; $\mathbf{F}_{xx} = \mathbf{D}_{xx}\mathbf{F}(a^0, 0)$ and $\mathbf{F}_{xxx} = \mathbf{D}_{xxx}\mathbf{F}(a^0, 0)$ are derivative matrices of \mathbf{F} . \mathbf{I} is the identity matrix.

The right side of equation (B1) includes several matrix products. For example, the first term is

$$\mathbf{u}\mathbf{F}_{xxx}vv\bar{v} = \sum_{l=1}^n \left(u_l \sum_{j,k,p=1}^n \frac{\partial^3 \mathbf{F}^l}{\partial x_j \partial x_k \partial x_p} v_j v_k \bar{v}_p \right).$$

For $\alpha'(0) > 0$, supercritical bifurcation takes place if $\delta'(0) > 0$, whereas subcritical bifurcation occurs if $\delta'(0) < 0$. In the former case, a stable periodic orbit bifurcates from $(\mathbf{x}, \gamma) = (a^0, 0)$ for $\gamma > 0$; in the latter case, an unstable orbit bifurcates from $(\mathbf{x}, \gamma) = (a^0, 0)$ for $\gamma < 0$.

In addition, due to $\delta'(0) = \gamma_2$ and $\eta'(0) = \tau_2$, one obtains $\text{Re } c_1(0) = -\delta'(0)\alpha'(0)$ and $\text{Im } c_1(0) = \Omega'(0)\delta'(0) + \Omega_c\eta'(0)$.

APPENDIX C: COEFFICIENTS OF $\mathbf{A}(\omega)$

$$a_1 = \frac{1}{\omega^2} [K_e + (k_1 x_0 + 1)K] + \frac{1}{\omega} (t_1 + k_1) D y_0 \tau - (1 + 2x t_1) m_f \tau^2, \quad a_2 = \frac{1}{\omega} (D_e + D).$$

$$a_3 = \frac{1}{\omega^2} k_2 K x_0 + \frac{1}{\omega} [(t_2 + k_2) y_0 + 1] D \tau - 2x_0 t_2 m_f \tau^2, \quad a_4 = 2m_f \tau.$$

$$b_1 = \frac{1}{\omega^2} k_1 K y_0 - \frac{1}{\omega} [(t_1 + k_1) x_0 + 1] D \tau - 2y_0 t_1 m_f \tau^2, \quad b_2 = -a_4.$$

$$b_3 = \frac{1}{\omega^2} [K_e + (k_2 y_0 + 1)K] - \frac{1}{\omega} (t_2 + k_2) x_0 D \tau - (2y_0 t_2 + 1) m_f \tau^2, \quad b_4 = a_2.$$

where

$$e_0 = \sqrt{x_0^2 + y_0^2}, \quad K = K_0(1 - e_0^2)^{-n}, \quad D = D_0(1 - e_0^2)^{-n}, \quad \tau = \tau_0(1 - e_0)^b,$$

$$k_1 = 2nx_0/(1 - e_0^2), \quad k_2 = 2ny_0/(1 - e_0^2), \quad t_1 = bx_0/e_0(1 - e_0),$$

$$t_2 = -by_0/e_0(1 - e_0).$$